Journal of Materials and Electronic Devices 2 (2021) 24-29


# Thermal and Structural Investigations of Cu-Al-Ni Shape Memory Alloys Irradiated Under Constant Gamma Radiation Dose

Ş. Nevin BALO, Abdulvahap ORHAN

Department of Physics, Faculty of Science, University of Firat, 23119 Elazig, Turkey

In this study, shape memory alloys (SMAs) (wt%) Cu-13.0Al-4Ni and Cu-13.5Al-4Ni were used. 40 kGy radiation dose gamma was applied to the alloy samples. The effects of radiation dose on CuAlNi SMA samples were investigated. The effects on thermodynamic parameters were determined by differential scanning calorimetry (DSC). Microstructural examinations were performed by X-ray diffraction (XRD) and optical microscopy observations. Microhardness measurements of homogeneous and irradiated samples with 40 kGy radiation dose were compared.

***Keywords:*** *Aging, Pressure, CuAlNi shape memory alloy, Microhardnes, Crystallite size.*

*Submission Date: 20 April 2021*
*Acceptance Date: 15 July 2021*

**Corresponding author: nbalo@firat.edu.tr.*

## 1. Introduction

Structural materials in reactor systems are predominantly crystalline metallic alloys. Almost all of the structural materials in reactors are metallic. Types of radiation that can change structural materials include neutrons, ions, electrons, and gamma rays. For these structures to fulfill their purpose, it is necessary to have a good understanding of the effect of radiation on materials to take into account the effects of radiation in the design, to reduce its effect by changing the operating conditions, or to create radiation-resistant materials that can better serve their purpose, and to serve as a guide. The operational safety of nuclear facilities can benefit from the use of smart material technologies in monitoring and inspection processes. The use of smart material technologies in such facilities can result in increased safety, reduced life-cycle costs, and increased performance while reducing personal exposure. However, the use of such smart materials in nuclear facilities requires knowledge of how materials respond to irradiation and how this response is affected by radiation dose. Shape memory alloys (SMAs) are in the smart material class. SMAs have been used as active alloys in mechanical devices for monitoring nuclear facilities [1-3].

Due to their superior properties, SMAs have found use in many different areas and have technological applications, as they enable to find extraordinary solutions to important engineering problems [4-7]. These alloys are alloys that can regain their original shape by diffusionless phase transformation (martensitic transformation) caused by the application of temperature and force separately or together [7,8]. This phase transformation gives physical and technological properties to metals and metal alloys. These properties are shape memory effect, thermoelasticity, and superelasticity [9-13]. Thermally excited SMAs undergo austenite↔martensite phase transformation at well-defined temperature ranges ($A_s$, $A_f$, $M_s$, $M_f$). Here, the subindexes A austenite, M martensite, s, and f indicate the starting and ending temperatures. Among the few existing alloy systems, equiatomic Ni-Ti alloys (nitinol) and Cu-based SMAs have received great attention. Cu-based shape memory alloys are also of great interest to researchers in practical applications

due to their low cost, good shape memory capabilities, and good damping properties [11,14-16].

Cu-based SMAs have an irregular structure of type A2 at high temperatures and enter a regular structure when cooled. In different SMAs, the ordered structures can be identified as B2, DO3, or L21, and these structures transform into martensite with further cooling [17,18]. CuAlNi SMAs exhibit different types of martensite such as 2H, 18R, and 6R depending on chemical composition, applied load, test temperature, and crystal orientation [6,19,20].

In this study, two different weight percent CuAlNi alloy were used. Alloys were irradiated with Co-60 gamma radiation source. The study was planned in two phases: (1) pre-irradiation measurements and (2) post-irradiation measurements. The aim here is to present different material properties to engineers for technological applications.

## 2. Material Method

The CuAlNi shape memory alloys used in this study were supplied from Recherche at TREFIMETAUX Center in France. The compositions of the alloy samples are given in Table-1. Piece samples cut from the alloys were subjected to heat treatment at a temperature in the β phase region determined from the equilibrium diagram of the CuAlNi alloy. The alloy samples were annealed in the β phase region at 930 ◦C for 30 minutes and then the samples were cooled rapidly in salty-ice water. Some of these examples, in Turkey Atomic Energy Agency Sarayköy Nuclear Research and Training Center (SANAEM) with a constant radiation dose (40 Gy) irradiated. The rate of the irradiation dose was set at 1273 Gy/h. The characteristic transformation temperatures and thermodynamic parameters of samples were determined by Perkin Elmer 8000 differential scanning calorimetry (DSC) with 10◦C/min heating/cooling rate. X-ray diffraction patterns of the alloy samples were taken with a Bruker AXS D8 Advance Model diffractometer in the range of 30◦ to 90◦. X-ray analyses of the alloy samples were performed using CuKα radiation at room temperature and the wavelength of the X-rays was 1.54060 Å. Following the polishing and chemical etching processes used on the alloy samples, optical microscope observations were made. Microhardness measurements were taken.

**Table 1.** Composition (wt%) of the investigated CuAlNi alloys.

| Alloy ID | Al (wt%) | Ni (wt%) |
|---|---|---|
| CAN1 | 13.0 | 4 |
| CAN2 | 13.5 | 4 |

## 3. Results

### *3.1. Differential scanning calorimetry (DSC) measurements*

DSC measurements of homogeneous samples and irradiated samples with a gamma radiation dose of 40 Gy were performed at a heating/cooling scan rate of 10 ◦C/min under atmospheric pressure in the appropriate temperature range. The transformation temperatures of the alloys are given in Table-2 and the thermodynamic parameters are given in Table-3. The transformation temperatures were determined by the tangent method. The equilibrium temperature between the forward and reverse transformation phases is determined by the equation below [21].

$$T_0 = (A_f + M_s)/2 \quad (1)$$

In the expression, $M_s$ is the martensite starting temperature and $A_f$ is the austenite ending temperature. The entropy change during the inverse transformation can be determined by the following equation [22].

$$\Delta S_{M\to A} = \Delta H_{M\to A}/T_0 \quad (2)$$

Here ΔS is entropy, ΔH is enthalpy and $T_0$ is the equilibrium temperature. DSC curves taken at 10 ◦C/min heating/cooling rates to observe the changes in thermodynamic parameters such as equilibrium temperature, enthalpy, and entropy of the applied irradiation are given in Fig.1. and Fig.2. The hysteresis in the transformation is represented by the temperature difference $T_0$-$M_s$. The $\Delta G^{A\to M}(M_s)$ Gibbs energy is characterized by the driving force for the nucleation of martensite in the austenite phase [23].

$$\begin{aligned}\Delta G^{A\to M}(M_s) &= \Delta G^{M\to A}(T_0) - \Delta G^{M\to A}(M_s)\\ &= -(T_0 - M_s)\Delta S^{M\to A}\end{aligned} \quad (3)$$

$M_f$-$M_s$' temperature difference is related to the elastic energy $G_E$ stored in the self-assembled martensitic variants and is given by the following expression.

$$\begin{aligned}\Delta G_E &= \Delta G^{A\to M}(M_s) - \Delta G^{A\to M}(M_f)\\ &= (M_s - M_f)\Delta S^{M\to A}\end{aligned} \quad (4)$$

Considering the homogeneous CAN1 and CAN2 alloy samples, the increase in the amount of aluminum decreased the equilibrium and transformation temperatures. Similarly, a decrease in thermodynamic parameters was also observed. It is clearly seen in Table-2 and Table-3 that the forward and reverse transformation temperatures and thermodynamic equilibrium temperatures of CAN1 and CAN2 samples irradiated with a fixed radiation dose of 40 kGy increased. The change in the thermodynamic parameters of the alloy

samples is given in Table-3. A decrease in enthalpy, entropy, and elasticity energy, which are the thermodynamic parameters of the CAN1 sample, is observed with irradiation, and a significant increase in Gibss free energy is observed. The changes in the thermodynamic parameters of the irradiated CAN2 sample are smaller and the elastic energy remained almost constant, while the Gibbs free energy increased slightly. Irradiation affected the enthalpy and entropy of the martensite and parent phase. This may be due to the influence of the crystallographic structure by irradiation.

**Table-2.** Transformation temperature of homogeneous (H) and irradiated (40kGy) CuAlNi SMA samples.

| Alloy ID | Process | $M_s$ (K) | $M_f$ (K ) | $A_s$ (K ) | $A_f$ (K) |
|---|---|---|---|---|---|
| CAN1 | H | 431,63 | 414,40 | 428,38 | 458,87 |
| CAN1 | 40 kGy | 434,78 | 419,09 | 433,96 | 463,62 |
| CAN2 | H | 334,27 | 318,42 | 341,22 | 354,18 |
| CAN2 | 40 kGy | 337,23 | 321,47 | 340,74 | 357,22 |

**Table-3.** Thermodynamic parameters of the homogeneous (H) and irradiated (40 kGy) CuAlNi SMA samples.

| Alloy ID | Process | $T_0$ (K) | $\Delta H^{M\rightarrow A}$ (J/kg) | $\Delta H^{A\rightarrow M}$ (J/kg) | $\Delta S^{M\rightarrow A}$ (J/kgK) | $\Delta S^{A\rightarrow M}$ (J/kgK) | $\Delta G_E$ (J/kg) | $\Delta G^{A\rightarrow M}$ (J/kg) |
|---|---|---|---|---|---|---|---|---|
| CAN1 | H | 445,25 | 12280,1 | -7514,3 | 27,58 | -16,87 | 475,20 | -375,63 |
| CAN1 | 40 kGy | 449,20 | 9156,8 | -10879,6 | 20,38 | -24,21 | 319,76 | -293,87 |
| CAN2 | H | 344,22 | 8437,8 | -5551,9 | 24,51 | -16,12 | 388,48 | -243,87 |
| CAN2 | 40 kGy | 347.22 | 8554,5 | -6694,5 | 24,63 | -19,28 | 388,16 | -246,05 |

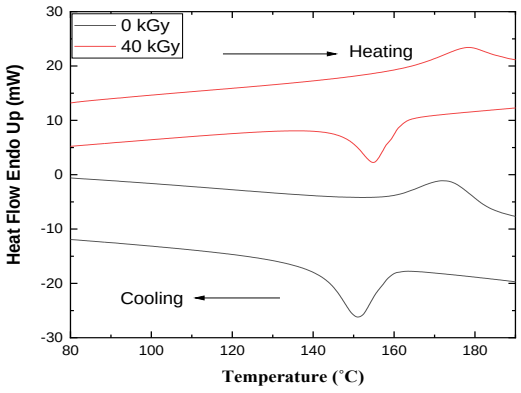


**Fig.1.** DSC curves of CAN1 samples irradiated with a homogeneous and 40 kGy gamma radiation dose.

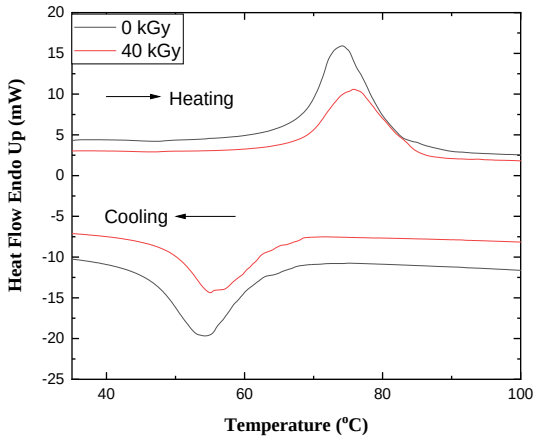


**Fig.2.** DSC curves of CAN2 samples irradiated with a homogeneous and 40 kGy gamma radiation dose.

### *3.2. X-ray diffraction (XRD) analysis results*

X-ray diffraction patterns of CAN1 and CAN2 shape memory alloy samples homogeneous and irradiated with constant gamma radiation dose are given in Fig.3. and Fig.4. There are peaks of martensite structure in CAN1 alloy samples the homogeneous and irradiated with a radiation dose of 40 kGy. A change was observed in the peak intensities with the applied radiation dose and some of the peaks disappeared and new martensite peaks were formed. In the XRD pattern of homogenous CAN2 SMA are peaks of the martensit phase (β' and γ') and γ2 precipitate phase. Depending on the composition, the CAN2 SMA underwent a combined transformation (β↔ β'+γ'). CuAlNi SMAs may undergo a combined transformation (β↔ β'+γ') depending on the composition [24-26]. In addition, it is thought that the $\gamma_2$ peak occurs depending on the cooling rate. Because when the cooling rate of the alloy is slow, $\gamma_2$ phases can easily precipitate in grains or grain boundaries [27]. A change was observed in the peak intensities of CAN2 alloy with the applied radiation dose.The crystallite size of homogeneous and irradiated alloy samples was calculated by Debye Scherrer equation [28-30].

$$D = \frac{0.9\lambda}{FWHM cos\theta}, \quad (5)$$

In the expression, D represents the crystallite size, λ the X-ray wavelength, FWHM the full width at half the maximum peak, and θ the Bragg angle. The changes in the crystallite

size of the alloys by irradiation are given in Table-4. When the homogeneous CAN1 and CAN2 alloy samples were compared, the crystal size increased due to the increase in the amount of Al. In addition, the crystal size of samples increased with irradiation in both sample

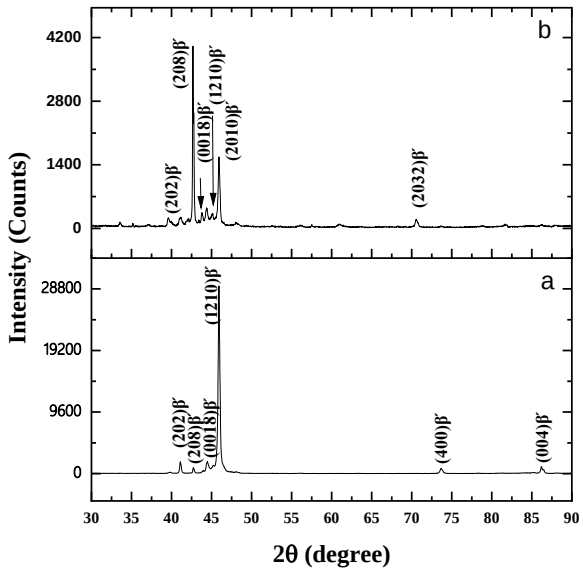


**Fig.3.** XRD patterns of CAN1 **(a)** homogenous sample **(b)** sample irradiated with 40 kGy gamma radiation dose.

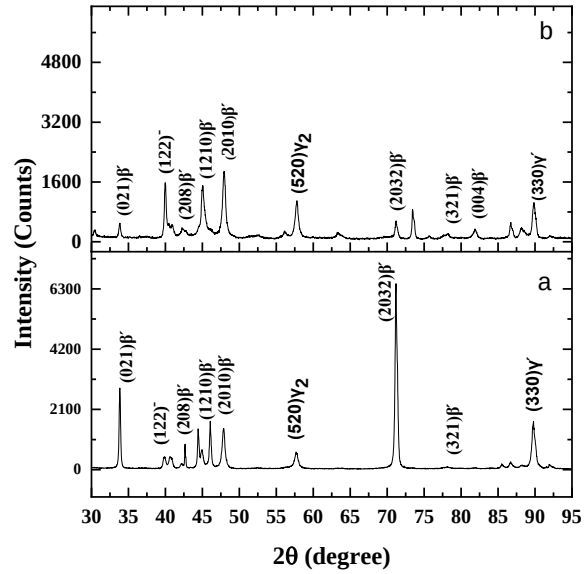


**Fig.4.** XRD patterns of CAN2 **(a)** homogenous sample **(b)** sample irradiated with 40 kGy gamma radiation dose.

### *3.3. Metallographic observations and microhardness results*

Optical photographs of CAN1 and CAN2 SMA samples homogeneous and irradiated with constant gamma radiation dose are given in Fig.5. and Fig.6. Fig.5. (a) and (b) show the optical photographs of CAN1 samples homogeneous and irradiated with 40 kGy gamma radiation dose, respectively, and Fig.6. (a) and (b) show the optical photographs of CAN2 samples homogeneous and irradiated with 40 kGy gamma radiation dose, respectively. As seen in Fig.5. (a) and Fig.6. (a), homogeneous CAN1 and CAN2 alloys are in polycrystalline structures. At room temperature, both are martensite in structure. The structure is composed of zigzag and needle-shaped martensites. As seen in Fig.5. (b) and Fig.6. (b) optical photographs of alloy samples irradiated with a radiation dose of 40 kGy, the structure is dominated by martensite plates. If the optical photograph of the irradiated CAN1 sample is compared to the photograph of the homogeneous sample at the same magnification, the grains enlarged slightly. Fewer grains and grain boundaries are seen in Fig.5. (b). Similar images for CAN2 are shown in Fig.6. (a) and (b). Average hardness values of alloy samples are given in Table-4. The average hardness results in the table also support the optical photographic results. The microhardness value decreased with the increase in grain size. Also, the microhardness of the homogeneous CAN1 sample is greater than the microhardness of the homogeneous CAN2. The grains seen in Fig.6. (a) are larger than the grains seen in Fig.5. (a). Therefore, its microhardness is also smaller. This is thought to be caused by the increase in the amount of aluminum.

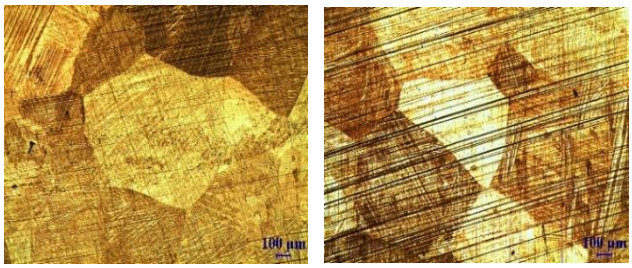


(a) (b)

**Fig.5.** Optical photograhps of CAN1 (a) homogeneous sample (b) sample irradiated with 40 kGy gamma radiation dose.

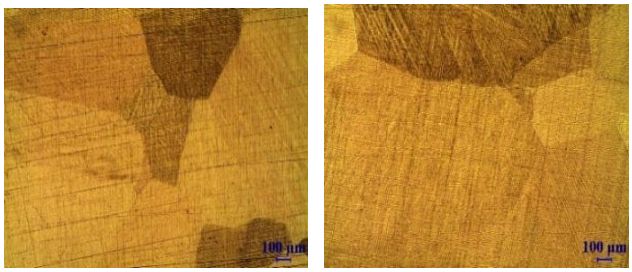


(a) (b)

**Fig.6.** Optical photograhps of CAN2 (a) homogeneous sample (b) sample irrasiated with 40 kGy gamma radiation dose.

**Table- 4.** Average microhardness values and crystallite sizes of CuAlNi shape memory alloys irradiated with homogeneous and constant gamma radiation dose.

| Alloys ID | Process | Avg. $HV_{0.1}$ Microhardness | Crystallite Size (nm) |
|---|---|---|---|
| CAN1 | Homogenous | 267,4 | 44,7306 |
| CAN1 | 40 kGy | 248,4 | 83,8693 |
| CAN2 | Homogenous | 255,2 | 48,1742 |
| CAN2 | 40 kGy | 252,4 | 51,9311 |

## 4. Conclusion

Cu-based SMAs are very sensitive to the content of alloying elements. The transformation temperatures of the CAN shape memory alloy decreased with the increase in the amount of aluminum.

The transformation temperatures and thermodynamic parameters of CAN1 and CAN2 alloy samples were affected by the applied irradiation. X-ray diffraction of homogeneous and irradiated CAN1 and CAN2 samples show peaks of martensite structure. Changes in peak intensities were observed with irradiation. Some peaks disappeared and new martensite peaks were formed. The crystallite size of the samples was also affected by the radiation dose. The change in crystallite size of CAN2 is smaller. The microhardness of the irradiated CAN2 alloy was also less affected.

The microhardness of irradiated CAN SMAs can be controlled by thermodynamic parameters (entropy, energy of elasticity) and crystal size.

### Acknowledgments

The study carried out was supported by Firat University Scientific Research Projects Unit (FÜBAP) under project number FF.19.09.

## References

**[1]** Grossbeck, M. L. Effect of radiation on strength and ductility of metals and alloys. (2012). 99-121

**[2]** Giurgiutiu, V., & Zagrai, A. N. Use of smart materials technologies in radiation environments and nuclear industry. In Smart Structures and Materials 2000: Smart Structures and Integrated Systems 3985. (2000) 855-866. International Society for Optics and Photonics. https://doi.org/10.1117/12.388812

**[3]** Was, G. S. Fundamentals of radiation materials science: metals and alloys. Springer (2016).

**[4]** Shelyakov, A. V., Sitnikov, N. N., Sheyfer, D. V., Borodako, K. A., Menushenkov, A. P., & Fominski, V. Y. The formation of the two-way shape memory effect in rapidly quenched TiNiCu alloy under laser radiation. Smart materials and structures, 24(11) (2015). 115031.

**[5]** Sutou, Y., Koeda, N., Omori, T., Kainuma, R., & Ishida, K. Effects of ageing on bainitic and thermally induced martensitic transformations in ductile Cu–Al–Mn-based shape memory alloys. Acta Materialia, 57(19) (2009) 5748-5758. https://doi.org/10.1016/j.actamat.2009.08.003

**[6]** Suresh, N., & Ramamurty, U. Effect of aging on mechanical behavior of single crystal Cu–Al–Ni shape memory alloys. Materials Science and Engineering: A, 454 (2007) 492-499. https://doi.org/10.1016/j.msea.2006.11.069

**[7]** Hartl, D. J., Mooney, J. T., Lagoudas, D. C., Calkins, F. T., & Mabe, J. H. Use of a Ni60Ti shape memory alloy for active jet engine chevron application: II. Experimentally validated numerical analysis. Smart Materials and Structures, 19(1) (2010) 015021. https:// doi:10.1088/0964-1726/19/1/015020

**[8]** Otsuka, K., & Wayman, C. M. (Eds.). Shape memory materials (1999) Cambridge university press.

**[9]** Recarte, V., Pérez-Landazábal, J. I., Rodríguez, P. P., Bocanegra, E. H., Nó, M. L., & San Juan, J. Thermodynamics of thermally induced martensitic transformations in Cu–Al–Ni shape memory alloys. Acta materialia, 52(13) (2004) 3941-3948. https://doi.org/10.1016/j.actamat.2004.05.009

**[10]** Straumal, B. B., Kilmametov, A. R., López, G. A., López-Ferreño, I., Nó, M. L., San Juan, J., ... & Baretzky, B. High-pressure torsion driven phase transformations in Cu–Al–Ni shape memory alloys. Acta Materialia, 125, (2017) 274-285. https://doi.org/10.1016/j.actamat.2016.12.003

**[11]** Balo, Ş. N., & Sel, N. Effects of thermal aging on transformation temperatures and some physical parameters of Cu–13.5 wt.% Al–4 wt.% Ni shape memory alloy. Thermochimica acta, 536, (2012) 1-5. https://doi.org/10.1016/j.tca.2012.02.007

**[12]** Said, Z., Necib, K., & Britah, A. Structural Characterization of Cu-13.58% Al-3.94% Ni (wt.%) shape memory alloy elaborated by fusion. In EPJ Web of Conferences 6, (2010) 29001). EDP Sciences. https://doi.org/10.1051/epjconf/20100629001

**[13]** Alaneme, K. K., Sulaimon, A. A., & Olubambi, P. A. Mechanical and corrosion behaviour of iron modified Cu-Zn-Al alloys. Acta Metallurgica Slovaca, 19(4), (2013) 292-301. https:// DOI 10.12776/ams.v19i4.184

**[14]** Li, M., Yan, S., Yan, W., & Shi, B. Effect of aging treatment on damping capacity in Cu–Al–Mn shape

memory alloy. Journal of Alloys and Compounds, 821, (2020) 153213. https://doi.org/10.1016/j.jallcom.2019.153213

**[15]** Dasgupta, R. A look into Cu-based shape memory alloys: Present scenario and future prospects. Journal of Materials Research, 29(16), (2014) 1681-1698. https://doi.org/10.1557/jmr.2014.189

**[16]** Balo, Ş. N., Ceylan, M., & Aksoy, M. Effects of deformation on the microstructure of a Cu–Al–Be shape memory alloy. Materials Science and Engineering: A, 311(1-2), (2001) 151-156. https://doi.org/10.1016/S0921-5093(01)00927-3

**[17]** Sarı, U., & Aksoy, I. Micro-structural analysis of self-accommodating martensites in Cu–11.92 wt% Al–3.78 wt% Ni shape memory alloy. Journal of Materials Processing Technology, 195(1-3), (2008) 72-76. https://doi.org/10.1016/j.jmatprotec.2007.04.116

**[18]** Canbay, C. A., & Polat, T. Thermal and structural alternations in CuAlMnNi shape memory alloy by the effect of different pressure applications. Physica B: Condensed Matter, 521, (2017) 331-338. https://doi.org/10.1016/j.physb.2017.07.017

**[19]** Shimizu, K., Sakamoto, H., & Otsuka, K. Phase diagram associated with stress-induced martensitic transformations in a Cu-Al-Ni alloy. Scripta Metallurgica, 12(9), (1978) 771-776. https://doi.org/10.1016/0036-9748(78)90033-9

**[20]** Aldırmaz, E., & Aksoy, I. Investigation of deformation and microstructure of bainite in Cu-9.97% Al-4.62% Mn alloy. Journal of Mining and Metallurgy, Section B: Metallurgy, 50(1), (2014) 87-90. DOI:10.2298/JMMB120704004A.

**[21]** Tong, H. C., & Wayman, C. M. Characteristic temperatures and other properties of thermoelastic martensites. Acta Metallurgica, 22(7), (1974) 887-896. https://doi.org/10.1016/0001-6160(74)90055-8

**[22]** Malimanek, J., & Zarubova, N. Calommetric investigation of the movement of phase interfaces in a Cu-Al-Ni single crystal. Scripta metallurgica et materialia, 32(9), (1995) 1347-1352.

**[23]** Romero, R., & Pelegrina, J. L. Change of entropy in the martensitic transformation and its dependence in Cu-based shape memory alloys. Materials Science and Engineering: A, 354(1-2), (2003) 243-250. https://doi.org/10.1016/S0921-5093(03)00013-3

**[24]** Pereira, E. C., Matlakhova, L. A., Matlakhov, A. N., de Araújo, C. J., Shigue, C. Y., & Monteiro, S. N., Reversible martensite transformations in thermal cycled polycrystalline Cu-13.7% Al-4.0% Ni alloy. Journal of Alloys and Compounds, 688, (2016) 436-446. https://doi.org/10.1016/j.jallcom.2016.07.210

**[25]** Izadinia, M., & Dehghani, K. Structure and properties of nanostructured Cu-13.2 Al-5.1 Ni shape memory alloy produced by melt spinning. Transactions of Nonferrous Metals Society of China, 21(9), (2011) 2037-2043. https://doi.org/10.1016/S1003-6326(11)60969-2

**[26]** Dora, T. R. K., Sampath, V., Li, Y., & Hodgson, P. In vitro cytotoxicity and corrosion studies of some copper base shape memory alloys. Materials Today: Proceedings, 4(10), (2017) 10672-10681. https://doi.org/10.1016/j.matpr.2017.08.013

**[27]** Wang, Z., Liu, X. F., & Xie, J. X. Effect of γ2 phase evolution on mechanical properties of continuous columnar-grained Cu–Al–Ni alloy. Materials Science and Engineering*:* A,*532*, (2012) 536-542. https://doi.org/10.1016/j.msea.2011.11.019

**[28]** Zu, X. T., Zhang, C. F., Zhu, S., Huo, Y., Wang, Z. G., & Wang, L. M. Electron irradiation-induced changes of martensitic transformation characteristics in a TiNiCu shape memory alloy.Materials Letters, 57(13-14), (2003) 2099-2103. https://doi.org/10.1016/S0167-577X(02)01145-X

**[29]** Aydın, C., El-Nasser, H. M., Yakuphanoglu, F., Yahia, I. S., & Aksoy, M. Nanopowder synthesis of aluminum doped cadmium oxide via sol–gel calcination processing. Journal of Alloys and Compounds, 509(3), (2011) 854-858. https://doi.org/10.1016/j.jallcom.2010.09.111

**[30]** Hoshiya, T., Takada, F., Ichihashi, Y., & Pak, H. R. Restoration phenomena of neutron-irradiated TiNi shape memory alloys. Materials Science and Engineering: A, 130(2), (1990) 185-191. https://doi.org/10.1016/0921-5093(90)90059-C